J. Math. Anal. Appl. 436 (2016) 692–717

Contents lists available at ScienceDirect

Journal of Mathematical Analysis and Applications

www.elsevier.com/locate/jmaa

Oscillations, fluctuation intensity and optimal harvesting of a bio-economic model in a complex habitat

Xue Zhang [a,b,*], Shuni Song [a], Jianhong Wu [b]

[a] College of Science, Northeastern University, Shenyang, Liaoning, 110819, China
[b] Center for Disease Modelling, York Institute for Health Research, York University, 4700 Keele Street, Toronto, ON, M3J 1P3, Canada

ARTICLE INFO

Article history:
Received 22 June 2015
Available online 21 December 2015
Submitted by J. Shi

Keywords:
Hopf bifurcation
Habitat complexity
Time delays
Stochastic behavior
Optimal harvesting

ABSTRACT

We investigate the effects of habitat complexity and multi-time delays on dynamics of a bio-economic predator–prey model. The differential–algebraic system theory is applied to transform the bio-economic model into a normal form, so that the local stability and existence of periodic solutions can be examined by varying the delays and the habitat complexity parameter. The direction of Hopf bifurcation and the stability of bifurcated periodic solutions are investigated. We also discuss the effect of fluctuating environment on dynamical behavior of a corresponding stochastic delayed-differential–algebraic system and derive expressions for intensities of population fluctuations. The model is also used to study the optimal harvesting strategy in order to maximize economic profit while sustaining the ecosystem. Numerical simulations are designed to illustrate the effectiveness of theoretical analysis.

1. Introduction

A predator–prey system, intensively studied in the literature (see [22,23,14,20]), is generally given by

$$\begin{cases} \dot{x}(t) = xg(x) - yf(x,y), \\ \dot{y}(t) = \beta yf(x,y) - dy, \end{cases} \tag{1}$$

where x and y denote the number of preys and predators, respectively. In the model, $g(x)$ is the per capita growth rate of the prey in the absence of predation. The trophic function $f(x,y)$ denotes the amount of prey caught by a predator per unit of time, β is the rate of conversion of nutrients from the prey into the reproduction of the predator and d is the mortality rate of the predator in the absence of prey.

* Corresponding author.
E-mail addresses: zhangxue@mail.neu.edu.cn (X. Zhang), songsn@126.com (S. Song), wujh@mathstat.yorku.ca (J. Wu).

http://dx.doi.org/10.1016/j.jmaa.2015.11.068
0022-247X/

There are different types of functional responses such as the prey-dependent type [25] (including the Holling I–III) and the predator-dependent type [12] (including the Beddinton–DeAngelis function and ratio-dependent response). It is also noted that (see [5,17,19]) habitat complexity can reduce the probability of capturing a prey by decreasing encounter rates between predator and prey. This led to incorporating the influence of habitat complexity into the Holling II [11] type functional response as follows:

$$f(x) = \frac{\alpha(1-\delta)x}{1+\alpha(1-\delta)\gamma x}, \tag{2}$$

where α and γ denote the attack coefficient and handing time for predation, respectively. The constant δ $(0 < \delta < 1)$ is a nondimensional parameter that reflects the strength of habitat complexity. When the habitat complexity is ignored, i.e., $\delta = 0$, the function (2) reduces to the classic Holling Type II functional response. Our work here is based on the aforementioned functional response.

It is well known that extensive and unregulated harvesting can cause species extinction, leading to the destruction of a natural predator–prey ecosystem. Regulated harvesting thus becomes a necessity to maintain an interactive biological system. However, such a regulation is always influenced by the cost-benefit of the harvesting activities. There has already an increasing body of literature for the modelling and analysis of bio-economic systems, often described by differential–algebraic equations (see, for example, [26,3,27,4,18] and references therein). In particular, in [26], a stage-structure differential–algebraic predator–prey system subject to harvesting is proposed to investigate the effects of harvesting on population dynamics. A singularly induced bifurcation leading to impulses and stability switch occurs at some critical point of economic interest, yielding rapid expansion of the predator. Zhang et al. [27] studied a ratio-dependent prey–predator singular model and analyzed the direction and stability of periodic solutions. However, this work ignored the fact that biological processes normally do not take place instantaneously due to the interaction with environment and other species, such as gestation, maturity and hunting. Chakraborty et al. [3] introduced a single discrete gestation delay in a differential–algebraic bio-economic system and established Hopf bifurcations in the neighborhood of coexisting equilibrium point. Liao et al. [15] investigated Hopf bifurcations of a three-species predator–prey system with two delays. In their study, it is possible to rescale the time to regard the sum of these two delays as a natural bifurcation parameter. This idea was also utilized by Song et al. [21] and Ma [16], while other relevant studies such as [24,8] simplified their analysis by requiring the two delays be identical. However, since the delays describing different ecological interaction are always different, it is important to discuss the impact of each delay independently on the dynamics, respectively.

In this paper, we study the following differential–algebraic bio-economic model with two time delays and habitat complexity:

$$\begin{cases} \dfrac{dx}{dt} = rx\left(1-\dfrac{x(t-\tau_1)}{K}\right) - \dfrac{\alpha(1-\delta)xy}{1+\alpha\gamma(1-\delta)x}, \\ \dfrac{dy}{dt} = \dfrac{\beta\alpha(1-\delta)x(t-\tau_2)y}{1+\alpha\gamma(1-\delta)x(t-\tau_2)} - dy - Ey, \\ E(py-w) - m = 0, \end{cases} \tag{3}$$

where $r > 0$ is the intrinsic growth rate of prey; $K > 0$ is the carrying capacity of prey; d is the intrinsic mortality rate of the predator species. We assume the prey dynamics is delayed by τ_1 due to slow replacement of resources and the predator takes time τ_2 to convert the food into its growth. In the model, the economics of harvesting is described by the algebraic equation, where E is the predator-dependent harvesting rate, $p > 0$ is the harvesting reward, Ew is the total fixed cost and $m > 0$ is the fixed profit.

The initial conditions for the predator–prey subsystem (3) are

$$(x|_{[-\tau,0]}, y|_{[-\tau,0]}) \in C_+([-\tau,0];\mathcal{R}_+^2)$$

with $\tau = \max\{\tau_1, \tau_2\}$; and when $y(0)$ is given, the initial value of $E(0)$ is given by $m/(py(0) - w)$, so we always assume that $y(0) > w/p$.

Our model considers three phenomena, oscillations, fluctuation intensity and optimal harvesting, all appearing in any predator–prey system. We start with the pure ecological consideration, and study the local stability and Hopf bifurcations by varying the self-limitation and gestation delay and the habitat complexity metric. We then address the impact of environmental variation on these dynamic behaviors by incorporating seasonality, temperature, sunshine and humidity, and the noise in the reproduction and mortality rate, and we establish the relationship between key ecological parameters such as time lags and fluctuation intensity for the model system to change its long-term behaviors. We finally address the issue of biological resources, by incorporating further harvesting policy. These considerations combined provide an integrative view how the predator–prey systems should be managed to scheme the delicate balance between optimal management of biological resources and sustainable development subject to uncertainty.

Our paper is organized as follows. In Section 2, we find the conditions for local stability and occurrence of Hopf bifurcations of system (3) around the interior equilibrium point in the presence of two delays. We discuss the direction of Hopf bifurcations and the stability of bifurcated periodic solutions by using the normal form theory and the center manifold theory in Section 3. In Section 4, we discuss the behavior of stochastic model and compute fluctuation intensity of populations. In Section 5, we consider the optimal harvesting strategy. Section 6 contains numerical simulations to illustrate the theoretical analysis, and Section 7 provides some additional remarks.

2. Local stability and Hopf bifurcation

Let $P(x^*, y^*, E^*)$ be the interior equilibrium of model system (3), where

$$E^* = \frac{m}{py^* - w},$$
$$y^* = \frac{r}{\alpha(1-\delta)}(1 - \frac{x^*}{K})(1 + \alpha\gamma(1-\delta)x^*),$$

and x^* satisfies the following equation:

$$H(x) := Ax^3 + Bx^2 + Cx + D = 0,$$

where

$$A = -\frac{\alpha\gamma pr}{K}(1-\delta)(\beta - \gamma d),$$
$$B = \frac{pr}{K}[(\beta - \gamma d)(\alpha(1-\delta)\gamma K - 1) + \gamma d],$$
$$C = (\beta - 2\gamma d)pr - \alpha(1-\delta)(m\gamma + w(\beta - \gamma d)) + \frac{prd}{\alpha K(1-\delta)},$$
$$D = -d(\frac{pr}{\alpha(1-\delta)} - w) - m.$$

In order to obtain the linearization of system (3), we introduce the following translation to reduce system (3) into state space form:

$$\begin{pmatrix} x \\ y \\ E \end{pmatrix} = \begin{pmatrix} 1 & 0 & 0 \\ 0 & 1 & 0 \\ 0 & -\dfrac{pE^*}{py^* - w} & 1 \end{pmatrix} \begin{pmatrix} x_1 \\ y_1 \\ E_1 \end{pmatrix},$$

and then we can rewrite system (3) as

$$\begin{cases} \dfrac{dx_1}{dt} = rx_1(1 - \dfrac{x_1(t-\tau_1)}{K}) - \dfrac{\alpha(1-\delta)x_1y_1}{1+\alpha\gamma(1-\delta)x_1}, \\ \dfrac{dy_1}{dt} = \dfrac{\beta\alpha(1-\delta)x_1(t-\tau_2)y_1}{1+\alpha\gamma(1-\delta)x_1(t-\tau_2)} - dy_1 - (E_1 - \dfrac{pE^*y_1}{py^* - w})y_1, \\ 0 = (E_1 - \dfrac{pE^*y_1}{py^* - w})(py_1 - w) - m. \end{cases} \tag{4}$$

We denote the corresponding interior equilibrium point of model (4) by $P_1(x_1^*, y_1^*, E_1^*)$, and transform the equilibrium point into zero by $x_1 = x_1^* + x_2$, $y_1 = y_1^* + y_2$ and $E_1 = E_1^* + l(x_2, y_2)$, where

$$l(x_2, y_2) = \frac{pE^*(y_1^* + y_2)}{py_1^* - w} + \frac{m}{p(y_1^* + y_2) - w} - \frac{pE^*y_1^*}{py_1^* - w} - E^*.$$

This transformation enables us to transform a differential–algebraic system to a system of differential equations for the new state variables (x_2, y_2) as follows:

$$\begin{cases} \dfrac{dx_2}{dt} = (x_2 + x_1^*)[r(1 - \dfrac{x_1^* + x_2(t-\tau_1)}{K}) - \dfrac{\alpha(1-\delta)(y_1^* + y_2)}{1+\alpha\gamma(1-\delta)(x_1^* + x_2)}], \\ \dfrac{dy_2}{dt} = (y_2 + y_1^*)[\dfrac{\beta\alpha(1-\delta)(x_1^* + x_2(t-\tau_2))}{1+\alpha\gamma(1-\delta)(x_1^* + x_2(t-\tau_2))} - d_2 - E^* - l(x_2, y_2) + \dfrac{pE^*(y_1^* + y_2)}{py_1^* - w}]. \end{cases} \tag{5}$$

The corresponding Jacobian matrix at the zero solution is given by

$$J = \begin{pmatrix} \dfrac{\alpha^2\gamma(1-\delta)^2x_1^*y_1^*}{(1+\alpha\gamma(1-\delta)x_1^*)^2} - \dfrac{rx_1^*}{K}e^{-\lambda\tau_1} & -\dfrac{\alpha(1-\delta)x_1^*}{1+\alpha\gamma(1-\delta)x_1^*} \\ \dfrac{(\beta\alpha(1-\delta)y_1^*}{(1+\alpha\gamma(1-\delta)x_1^*)^2}e^{-\lambda\tau_2} & \dfrac{pE^*y_1^*}{py_1^* - w} \end{pmatrix}.$$

The characteristic equation is given by

$$\lambda^2 + A_1\lambda + A_2 + (A_3\lambda + A_4)e^{-\lambda\tau_1} + A_5e^{-\lambda\tau_2} = 0, \tag{6}$$

where

$$\begin{aligned} A_1 &= -\frac{\alpha^2\gamma(1-\delta)^2x_1^*y_1^*}{(1+\alpha\gamma(1-\delta)x_1^*)^2} - \frac{pE^*y_1^*}{py_1^* - w}, \\ A_2 &= \frac{p\alpha^2\gamma(1-\delta)^2x_1^*y_1^{*2}E^*}{(1+\alpha\gamma(1-\delta)x_1^*)^2(py_1^* - w)}, \\ A_3 &= \frac{rx_1^*}{K}, \\ A_4 &= -\frac{rx_1^*y_1^*E^*}{K(py_1^* - w)}, \\ A_5 &= \frac{\beta\alpha^2(1-\delta)^2x_1^*y_1^*}{(1+\alpha\gamma(1-\delta)x_1^*)^3}. \end{aligned}$$

In the case where $\tau_1 = \tau_2 = 0$, the characteristic equation (6) becomes

$$\lambda^2 + (A_1 + A_3)\lambda + A_2 + A_4 + A_5 = 0.$$

Thus from the Routh–Hurwitz criteria, the interior equilibrium of model (4) in the absence of time delay is locally asymptotically stable if the following conditions are satisfied:

$$A_1 + A_3 > 0 \quad \text{and} \quad A_2 + A_4 + A_5 > 0. \tag{7}$$

Now, we discuss the effects of the two time delays on the stability at the positive equilibrium point P_1 in the following four cases.

Case 1. $\tau_1 = 0$ and $\tau_2 > 0$.

In this case, the equation (6) can be reduced into

$$\lambda^2 + (A_1 + A_3)\lambda + (A_2 + A_4) + A_5 e^{-\lambda\tau_2} = 0. \tag{8}$$

If $i\omega_2(\omega_2 > 0)$ is a root of equation (8), then

$$-\omega_2^2 + (A_1 + A_3)i\omega_2 + A_2 + A_4 + A_5 e^{-i\omega_2\tau_2} = 0.$$

Separating the real and imaginary parts, we obtain

$$\begin{cases} -\omega_2^2 + A_2 + A_4 = -A_5\cos(\omega_2\tau_2), \\ (A_1 + A_3)\omega_2 = A_5\sin(\omega_2\tau_2), \end{cases} \tag{9}$$

from which we have

$$\omega_2^4 + ((A_1 + A_3)^2 - 2(A_2 + A_4))\omega_2^2 + (A_2 + A_4)^2 - A_5^2 = 0. \tag{10}$$

There is a unique positive real root ω_{20} satisfying the above equation if (7) holds and the following condition is satisfied:

$$A_2 + A_4 - A_5 < 0. \tag{11}$$

The corresponding $\tau_{2k} > 0$ such that the characteristic equation (8) has a pair of purely imaginary roots $\pm i\omega_{20}$ are given by

$$\tau_{2k} = \frac{1}{\omega_{20}}\arccos\frac{-\omega_{20}^2 + A_2 + A_4}{-A_5} + \frac{2k\pi}{\omega_{20}}, \quad k = 0, 1, 2, \cdots. \tag{12}$$

If $A_2 + A_4 - A_5 > 0$, equation (10) has no real root and the interior equilibrium of model (3) is asymptotically stable for any time delay $\tau_2 > 0$.

Differentiating both sides of (8) with respect to τ_2 yields

$$sign\left(\frac{d}{d\tau_2}Re(\lambda)\right)|_{\tau_{2k}} = sign\left(\frac{\omega^4 - (A_2 + A_4)^2 + A_5^2}{(A_1 + A_3 + \tau_{2k}(A_2 + A_4 - \omega_{20}^2))^2 + \omega_{20}^2(2 + \tau_{2k}(A_1 + A_3))^2}\right) > 0.$$

Theorem 1. *Let (7), (11) hold and define* $\tau_{20} > 0$ *as*

$$\tau_{20} = \frac{1}{\omega_{20}}\arccos\frac{-\omega_{20}^2 + u_1u_4}{u_2u_3}.$$

The positive equilibrium P *of model (3) is locally asymptotically stable for* $\tau_2 < \tau_{20}$ *and there undergoes a Hopf bifurcation at* P *when* $\tau_2 = \tau_{20}$. *That is, the model (3) has a branch of periodic solutions bifurcating from the positive equilibrium* P *near* $\tau_2 = \tau_{20}$.

Case 2. $\tau_1 > 0$ and $\tau_2 = 0$.

Using a similar analysis as in the Case 1, we can obtain the following result:

Theorem 2. *Assume that (7) holds and $A_2 + A_5 - A_4 < 0$. Let ω_{10} be the unique positive real root satisfying the following equation:*

$$\omega^4 + (A_1^2 - 2A_2 - A_3^2 - 2A_5)\omega^2 + (A_2 + A_5)^2 - A_4^2 = 0$$

and

$$\tau_{10} = \frac{1}{\omega_{10}} \arccos \frac{(A_4 - A_1A_3)\omega_{10}^2 - A_4(A_2 + A_5)}{A_4^2 + A_3^3\omega_{10}^2}.$$

Then the positive equilibrium P of model (3) is locally asymptotically stable for $\tau_1 < \tau_{10}$, and there undergoes a Hopf bifurcation at $\tau_1 = \tau_{10}$.

Case 3. $\tau_1 > 0$ and $\tau_2 \in (0, \tau_{20})$.

In this case, we consider τ_1 as a parameter and τ_2 being in the stable interval $(0, \tau_{20})$. Assume that, for some $\tau_1 > 0$, $\lambda = i\omega$ is a root of the equation (6), where ω is a positive real number. If we substitute $i\omega$ into (6) and separate the real and imaginary parts, then we obtain the following transcendental equations:

$$\begin{cases} -\omega^2 + A_2 + A_5\cos(\omega\tau_2) = -A_4\cos(\omega\tau_1) - A_3\omega\sin(\omega\tau_1), \\ A_1\omega - A_5\sin(\omega\tau_2) = -A_3\omega\cos(\omega\tau_1) + A_4\sin(\omega\tau_1), \end{cases} \tag{13}$$

from which it follows that

$$\begin{aligned} &\omega^4 + [A_1^2 - A_3^2 - 2A_2 - 2A_5\cos(\omega\tau_2)]\omega^2 - 2A_1A_5\omega\sin(\omega\tau_2) \\ &\quad + A_2^2 - A_4^2 + A_5^2 + 2A_2A_5\cos(\omega\tau_2) = 0. \end{aligned} \tag{14}$$

The equation (14) has a positive real root ω_{10}^* if the condition $(A_2 + A_5)^2 < A_4^2$ holds. In addition, equation (13) can also be rewritten as

$$\begin{cases} A_5\cos(\omega\tau_2) = -A_4\cos(\omega\tau_1) - A_3\omega\sin(\omega\tau_1) + \omega^2 - A_2, \\ -A_5\sin(\omega\tau_2) = -A_3\omega\cos(\omega\tau_1) + A_4\sin(\omega\tau_1) - A_1\omega. \end{cases} \tag{15}$$

We define

$$\begin{aligned} \tau_{1k}^* &= \frac{1}{\omega_{10}^*}\left[\arccos \frac{(\omega_{10}^{*2} - A_2)^2 + (A_1^2 + A_3^2)\omega_{10}^{*2} + A_4^2 - A_5^2}{2\sqrt{A_4^2 + A_3^2\omega_{10}^{*2}}\sqrt{(\omega_{10}^{*2} - A_2)^2 + A_1^2\omega_{10}^{*2}}} - \phi_1 + \phi_2\right] + \frac{2k\pi}{\omega_{10}^*}, \\ k &= 0, 1, 2, \cdots, \end{aligned}$$

where

$$\begin{aligned} \phi_1 &= \arctan \frac{A_4}{A_3\omega_{10}^*}, \\ \phi_2 &= \arctan \frac{\omega_{10}^{*2} - A_2}{A_1\omega_{10}^*}. \end{aligned}$$

Using the Butler's Lemma [7], it can be concluded that the interior positive equilibrium P_1 remains stable for $\tau_1 < \tau_{10}^*$. We now examine whether the system (3) undergoes a Hopf bifurcation phenomenon at P when τ_1 increases through τ_{10}^*.

Differentiating (6) with respect to τ_1 and substituting the eigenvalue $i\omega_{10}^*$ and time delay $\tau_1 = \tau_{10}^*$, we obtain that

$$\begin{aligned} U\left(\frac{d(Re\,\lambda)}{d\tau_1}\right)|_{\tau_{10}^*} + V\left(\frac{d\omega}{d\tau_1}\right)|_{\tau_{10}^*} = R, \\ -V\left(\frac{d(Re\,\lambda)}{d\tau_1}\right)|_{\tau_{10}^*} + U\left(\frac{d\omega}{d\tau_1}\right)|_{\tau_{10}^*} = S, \end{aligned} \tag{16}$$

where

$$\begin{aligned} U &= A_1 + A_3\cos\omega_{10}^*\tau_{10}^* - \tau_{10}^*(A_4\cos\omega_{10}^*\tau_{10}^* + A_3\omega_{10}^*\sin\omega_{10}^*\tau_{10}^*) \\ &\quad - A_5\tau_2\cos\omega_{10}^*\tau_2, \\ V &= -2\omega_{10}^* + A_3\sin\omega_{10}^*\tau_{10}^* + \tau_{10}^*(A_3\omega_{10}^*\cos\omega_{10}^*\tau_{10}^* + -A_4\sin\omega_{10}^*\tau_{10}^*) \\ &\quad - A_5\tau_2\sin\omega_{10}^*\tau_2, \\ R &= -\omega_{10}^*(A_3\omega_{10}^*\cos\omega_{10}^*\tau_{10}^* - A_4\sin\omega_{10}^*\tau_{10}^*), \\ S &= \omega_{10}^*(A_3\omega_{10}^*\sin\omega_{10}^*\tau_{10}^* + A_4\cos\omega_{10}^*\tau_{10}^*). \end{aligned}$$

From these equations, we conclude that

$$\left(\frac{d(Re\,\lambda)}{d\tau_1}\right)|_{\tau_{10}^*} = \frac{UR - VS}{U^2 + V^2} \neq 0.$$

Therefore, we can obtain:

Theorem 3. *Assume that (7) and the condition* $(A_2 + A_5)^2 < A_4^2$ *hold. Then the positive equilibrium* P *of model (3) is locally asymptotically stable for* $\tau_1 \in [0, \tau_{10}^*)$ *and there undergoes Hopf bifurcation when* $\tau_1 = \tau_{10}^*$, *where*

$$\tau_{10}^* = \frac{1}{\omega_{10}^*}[\arccos\frac{(\omega_{10}^{*2} - A_2)^2 + (A_1^2 + A_3^2)\omega_{10}^{*2} + A_4^2 - A_5^2}{2\sqrt{A_4^2 + A_3^2\omega_{10}^{*2}}\sqrt{(\omega_{10}^{*2} - A_2)^2 + A_1^2\omega_{10}^{*2}}} - \phi_1 + \phi_2],$$

where $\phi_1 = \arctan\dfrac{A_4}{A_3\omega_{10}^*}$, $\phi_2 = \arctan\dfrac{\omega_{10}^{*2} - A_2}{A_1\omega_{10}^*}$.

Case 4. $\tau_1 \in (0, \tau_{10})$ and $\tau_2 > 0$.

Using a similar analysis as in the Case 3, we can obtain:

Theorem 4. *Assume that (7) and* $(A_2 + A_4)^2 < A_5^2$ *hold. Let* ω_{20}^* *be a positive real root satisfying the following equation:*

$$\begin{aligned} \omega^4 &- 2A_3\sin(\omega\tau_1)\omega^3 + [A_1^2 + A_3^2 - 2A_2 + 2(A_1A_3 - A_4)\cos(\omega\tau_1)]\omega^2 \\ &+ 2(A_2A_3 - A_1A_4)\sin(\omega\tau_1)\omega + A_2^2 + A_4^2 + 2A_2A_4\cos(\omega\tau_1) - A_5^2 = 0, \end{aligned}$$

and

$$\tau_{20}^* = \frac{1}{\omega_{20}*}[\arccos\frac{(-\omega_{20}^{*2} + A_2)^2 + (A_1^2 - A_3^2)^2\omega_{20}^{*2} + +A_5^2 - A_4^2}{-2A_5\sqrt{A_1^2\omega_{20}^{*2} + (-\omega_{20}^{*2} + A_2)^2}} - \psi],$$

where $\psi = \arctan \dfrac{A_1\omega_{20}^*}{-\omega_{20}^{*2} + A_2}$. *Then the positive equilibrium* P *of model (3) is locally asymptotically stable for* $\tau_2 \in [0, \tau_{20}^*)$, *and there undergoes Hopf bifurcation at* $\tau_2 = \tau_{20}^*$.

3. Stability of bifurcated periodic solutions

In this section, we consider the direction of Hopf bifurcation, stability and period of the periodic solution bifurcating from the positive equilibrium P. Following the ideas of Hassard et al. [10], we derive the explicit formulae for determining these properties of Hopf bifurcation at the critical value τ_{10}^* for fixed $\tau_2^* \in (0, \tau_{20})$ by employing the normal form method and center manifold theorem. Without loss of generality, in this section we assume that $\tau_2^* < \tau_{10}^*$. Let

$$u_1 = x_2 - x_2^*,$$
$$u_2 = y_2 - y_2^*,$$

and $u_1(t) = x_2(\tau_1 t)$, $u_2(t) = y_2(\tau_1 t)$, $\tau_1 = \tau_{10}^* + \mu$, $\mu \in R$. Then $\mu = 0$ is the Hopf bifurcation value of system (5). Next, we work in the fixed phase space $C = C([-1, 0], R^2)$. In space C, system (5) is transformed into an FDE as

$$\dot{u}(t) = L_\mu(u_t) + F(\mu, u_t), \tag{17}$$

where $u(t) = (u_1(t), u_2(t))^T \in R^2$, and $L_\mu : C \to R$, $F : R \times C \to R$ are given respectively by

$$\begin{aligned} L_\mu(\phi) = (\tau_{10}^* + \mu)\Bigg(& \begin{pmatrix} \dfrac{\alpha^2\gamma(1-\delta)^2 x_1^* y_1^*}{(1+\alpha\gamma(1-\delta)x_1^*)^2} & -\dfrac{\alpha(1-\delta)x_1^*}{1+\alpha\gamma(1-\delta)x_1^*} \\ 0 & \dfrac{pE_1^* y_1^*}{py_1^* - w} \end{pmatrix} \phi(0) \\ & + \begin{pmatrix} 0 & 0 \\ \dfrac{\beta\alpha(1-\delta)y_1^*}{(1+\alpha\gamma(1-\delta)x_1^*)^2} & 0 \end{pmatrix} \phi(-\tfrac{\tau_2^*}{\tau_{10}^*}) + \begin{pmatrix} -\dfrac{rx_1^*}{K} & 0 \\ 0 & 0 \end{pmatrix} \phi(-1)\Bigg) \end{aligned} \tag{18}$$

and

$$F(\mu, \phi) = (\tau_{10}^* + \mu) \begin{pmatrix} \dfrac{\alpha^2\gamma(1-\delta)^2 y_1^*}{(1+\alpha\gamma(1-\delta)x_1^*)^3}\phi_1^2(0) - \dfrac{\alpha(1-\delta)}{(1+\alpha\gamma(1-\delta)x_1^*)^2}\phi_1(0)\phi_2(0) \\ -\dfrac{r}{K}\phi_1(0)\phi_1(-1) - \dfrac{\alpha^3\gamma^2(1-\delta)^3 y_1^*}{(1+\alpha\gamma(1-\delta)x_1^*)^4}\phi_1^3(0) \\ +\dfrac{\alpha^2\gamma(1-\delta)^2}{(1+\alpha\gamma(1-\delta)x_1^*)^3}\phi_1^2(0)\phi_2(0) + \cdots \\ -\dfrac{\beta\alpha^2\gamma(1-\delta)^2 y_1^*}{(1+\alpha\gamma(1-\delta)x_1^*)^3}\phi_1^2(-\dfrac{\tau_2^*}{\tau_{10}^*}) + \dfrac{\beta\alpha(1-\delta)}{(1+\alpha\gamma(1-\delta)x_1^*)^2} \\ \cdot \phi_1(-\dfrac{\tau_2^*}{\tau_{10}'})\phi_2(0) - \dfrac{mpw}{(py_1^* - w)^3}\phi_2^2(0) + \dfrac{\beta\alpha^3\gamma^2(1-\delta)^3 y_1^*}{(1+\alpha\gamma(1-\delta)x_1^*)^4} \\ \cdot \phi_1^3(-\dfrac{\tau_2^*}{\tau_{10}^*}) - \dfrac{\beta\alpha^2\gamma(1-\delta)^2}{(1+\alpha\gamma(1-\delta)x_1^*)^3}\phi_1^2(-\dfrac{\tau_2^*}{\tau_{10}^*})\phi_2(0) \\ +\dfrac{mp^2 w}{(py_1^* - w)^4}\phi_2^3(0) + \cdots \end{pmatrix}, \tag{19}$$

where $\phi(\theta) = (\phi_1(\theta), \phi_2(\theta))^T \in C$.

By the Riesz representation theorem, there exists a 2×2 matrix $\eta(\theta,\mu)$ of bounded variation for $\theta\in[-1,0]$, such that

$$L_\mu\phi=\int_{-1}^{0}d\eta(\theta,\mu)\phi(\theta),\quad \text{for}\quad \phi\in C.$$

In fact, we can choose

$$\eta(\theta,\mu)=\begin{cases}(\tau_{10}^*+\mu)\begin{pmatrix}\dfrac{\alpha^2\gamma(1-\delta)^2x_1^*y_1^*}{(1+\alpha\gamma(1-\delta)x_1^*)^2}-\dfrac{rx_1^*}{K} & \dfrac{-\alpha(1-\delta)x_1^*}{1+\alpha\gamma(1-\delta)x_1^*}\\ \dfrac{\beta\alpha(1-\delta)y_1^*}{(1+\alpha\gamma(1-\delta)x_1^*)^2} & \dfrac{pE_1^*y_1^*}{py_1^*-w}\end{pmatrix}, & \theta=0,\\ (\tau_{10}^*+\mu)\begin{pmatrix}-\dfrac{rx_1^*}{K} & 0\\ \dfrac{\beta\alpha(1-\delta)\gamma y_1^*}{(1+\alpha\gamma(1-\delta)x_1^*)^2} & 0\end{pmatrix}, & \theta\in[-\dfrac{\tau_2^*}{\tau_{10}^*},0),\\ (\tau_{10}^*+\mu)\begin{pmatrix}-\dfrac{rx_1^*}{K} & 0\\ 0 & 0\end{pmatrix}, & \theta\in(-1,-\dfrac{\tau_2^*}{\tau_{10}^*}),\\ 0_{2\times2}, & \theta=-1.\end{cases}$$

For $\phi\in C^1([-1,0],R^2)$, define

$$A(\mu)\phi=\begin{cases}\dfrac{d\phi(\theta)}{d\theta}, & -1\le\theta<0,\\ \int_{-1}^{0}d\eta(s,\mu)\phi(s), & \theta=0,\end{cases}$$

and

$$R(\mu)\phi=\begin{cases}0, & -1\le\theta<0,\\ F(\mu,\phi), & \theta=0.\end{cases}$$

Then system (17) is equivalent to

$$\dot{u}_t=A(\mu)u_t+R(\mu)u_t,\tag{20}$$

where $u_t(\theta)=u(t+\theta)$ for $\theta\in[-1,0]$.

For $\psi\in C^1([0,1],(R^2)^*)$, define

$$A^*\psi(s)=\begin{cases}-\dfrac{d\psi(s)}{ds}, & s\in(0,1],\\ \int_{-1}^{0}d\eta^T(t,0)\psi(-t), & s=0,\end{cases}$$

and the bilinear form

$$\langle\psi(s),\phi(\theta)\rangle=\overline{\psi}(0)\phi(0)-\int_{-1}^{0}\int_{\xi=0}^{\theta}\overline{\psi}(\xi-\theta)d\eta(\theta)\phi(\xi)d\xi,\tag{21}$$

where $\eta(\theta)=\eta(\theta,0)$. Then $A=A(0)$ and A^* are adjoint operators.

Since $\pm i\omega_{10}^*\tau_{10}^*$ are eigenvalues of $A(0)$, they are also eigenvalues of A^*. Next, we need to compute the eigenvector of $A(0)$ and A^* corresponding to $i\omega_{10}^*\tau_{10}^*$ and $-i\omega_{10}^*\tau_{10}^*$, respectively.

Suppose that $q(\theta) = (1, \Delta)^T e^{i\omega_{10}^*\tau_{10}^*\theta}$ is the eigenvector of $A(0)$ corresponding to $i\omega_{10}^*\tau_{10}^*$, then $A(0)q(\theta) = i\omega_{10}^*\tau_{10}^* q(\theta)$. The definition of $A(0)$ and $\eta(\theta, \mu)$ yields

$$\begin{pmatrix} \dfrac{\alpha^2\gamma(1-\delta)^2x_1^*y_1^*}{(1+\alpha\gamma(1-\delta)x_1^*)^2} - \dfrac{rx_1^*}{K}e^{-i\omega_{10}^*\tau_{10}^*} & -\dfrac{\alpha(1-\delta)x_1^*}{1+\alpha\gamma(1-\delta)x_1^*} \\ \dfrac{\beta\alpha(1-\delta)y_1^*}{(1+\alpha\gamma(1-\delta)x_1^*)^2}e^{-i\omega_{10}^*\tau_2^*} & \dfrac{pE_1^*y_1^*}{py_1^*-w} \end{pmatrix} q(0) = i\omega_{10}^* q(0).$$

Then we can obtain

$$\Delta = \frac{i\omega_{10}^* + \dfrac{rx_1^*}{K}e^{-i\omega_{10}^*\tau_{10}^*} - \dfrac{\alpha^2\gamma(1-\delta)^2x_1^*y_1^*}{(1+\alpha\gamma(1-\delta)x_1^*)^2}}{-\dfrac{\alpha(1-\delta)x_1^*}{1+\alpha\gamma(1-\delta)x_1^*}}.$$

Similarly, let $q^*(s) = D(1, \Delta^*)e^{i\omega_{10}^*\tau_{10}^* s}$ be the eigenvector of A^* corresponding to $-i\omega_{10}^*\tau_{10}^*$, we can obtain

$$\Delta^* = \frac{-i\omega_{10}^* + \dfrac{rx_1^*}{K}e^{i\omega_{10}^*\tau_{10}^*} - \dfrac{\alpha^2\gamma(1-\delta)^2x_1^*y_1^*}{(1+\alpha\gamma(1-\delta)x_1^*)^2}}{\dfrac{\beta\alpha(1-\delta)y_1^*}{(1+\alpha\gamma(1-\delta)x_1^*)^2}e^{i\omega_{10}^*\tau_2^*}}.$$

By (21) we get

$$\begin{aligned} &\langle q^*(s), q(\theta)\rangle \\ &= \overline{D}(1, \overline{\Delta^*})(1, \Delta)^T - \int_{-1}^{0}\int_{\xi=0}^{\theta} \overline{D}(1, \overline{\Delta^*})e^{-i\omega_{10}^*\tau_{10}^*(\xi-\theta)}d\eta(\theta)(1, \Delta)^T e^{i\omega_{10}^*\tau_{10}^*\xi}d\xi \\ &= \overline{D}\left(1 + \overline{\Delta^*}\Delta - \frac{rx_1^*}{K}e^{-i\omega_{10}^*\tau_{10}^*} + \frac{\beta\alpha(1-\delta)y_1^*\tau_2^*\overline{\Delta^*}}{\tau_{10}^*(1+\alpha\gamma(1-\delta)x_1^*)^2}e^{-i\omega_{10}^*\tau_2^*}\right). \end{aligned}$$

Then we obtain

$$\overline{D} = \left(1 + \overline{\Delta^*}\Delta - \frac{rx_1^*}{K}e^{-i\omega_{10}^*\tau_{10}^*} + \frac{\beta\alpha(1-\delta)y_1^*\tau_2^*\overline{\Delta^*}}{\tau_{10}^*(1+\alpha\gamma(1-\delta)x_1^*)^2}e^{-i\omega_{10}^*\tau_2^*}\right)^{-1}.$$

Clearly, the conditions $\langle q^*(s), q(\theta)\rangle = 1$ and $\langle q^*(s), \overline{q}(\theta)\rangle = 0$ are satisfied. Let u_t be the solution of (20) when $\mu = 0$. Define

$$\begin{aligned} z(t) &= \langle q^*, u_t\rangle, \\ W(t, \theta) &= u_t(\theta) - 2\,Re\{z(t)q(\theta)\}. \end{aligned} \tag{22}$$

On the center manifold C_0, we have

$$W(t, \theta) = W(z(t), \overline{z}(t), \theta),$$

and

$$W(z(t),\overline{z}(t),\theta)=W_{20}(\theta)\frac{z^2}{2}+W_{11}(\theta)z\overline{z}+W_{02}(\theta)\frac{\overline{z}^2}{2}+\cdots, \tag{23}$$

where z and $\overline{z}$ are local coordinates for center manifold C_0 in the direction of q^* and $\overline{q^*}$. Note that W is real if u_t is real. We only consider real solutions. For solution $u_t\in C_0$ of (20), since $\mu=0$, we have

$$\begin{aligned}\dot{z}(t)&=i\omega_{10}^*\tau_{10}^*z+\overline{q^*}(0)F(0,W(z,\overline{z},0)+2\,Re\{z(t)q(\theta)\})\rangle\\&=i\omega_{10}^*\tau_{10}^*z+\overline{q^*}(0)F_0(z,\overline{z}).\end{aligned}$$

We rewrite this equation as

$$\dot{z}(t)=i\omega_{10}^*\tau_{10}^*z+g(z,\overline{z}),$$

where

$$\begin{aligned}g(z,\overline{z})&=\overline{q^*}(0)F_0(z,\overline{z})\\&=g_{20}(\theta)\frac{z^2}{2}+g_{11}(\theta)z\overline{z}+g_{02}(\theta)\frac{\overline{z}^2}{2}+g_{21}(\theta)\frac{z^2\overline{z}}{2}+\cdots.\end{aligned} \tag{24}$$

From (22) and (23), we have

$$\begin{aligned}u_t&=(u_{1t}(\theta),u_{2t}(\theta))\\&=W(t,\theta)+2\,Re\{z(t)q(\theta)\},\end{aligned}$$

where $q(\theta)=(1,\Delta)^Te^{i\omega_{10}^*\tau_{10}^*\theta}$, then

$$\begin{aligned}u_{1t}(0)&=W^{(1)}(t,0)+z+\overline{z},\\u_{2t}(0)&=W^{(2)}(t,0)+\Delta z+\overline{\Delta}\overline{z},\end{aligned}$$

$$\begin{aligned}u_{1t}(-\frac{\tau_2^*}{\tau_{10}^*})&=W^{(1)}(t,-\frac{\tau_2^*}{\tau_{10}^*})+ze^{-i\omega_{10}^*\tau_2^*}+\overline{z}e^{i\omega_{10}^*\tau_2^*},\\u_{2t}(-\frac{\tau_2^*}{\tau_{10}'})&=W^{(2)}(t,-\frac{\tau_2^*}{\tau_{10}'})+\Delta ze^{-i\omega_{10}^*\tau_2^*}+\overline{\Delta}\overline{z}e^{i\omega_{10}^*\tau_2^*},\end{aligned}$$

$$\begin{aligned}u_{1t}(-1)&=W^{(1)}(t,-1)+ze^{-i\omega_{10}^*\tau_{10}^*}+\overline{z}e^{i\omega_{10}^*\tau_{10}^*},\\u_{2t}(-1)&=W^{(2)}(t,-1)+\Delta ze^{-i\omega_{10}^*\tau_{10}^*}+\overline{\Delta}\overline{z}e^{i\omega_{10}^*\tau_{10}^*}.\end{aligned}$$

It follows, together with (19), the following expression:

$$g(z,\overline{z})=\overline{q^*}(0)F_0(z,\overline{z}).$$

Comparing the coefficients with (24), we have

$$\begin{aligned}g_{20}=2\overline{D}\tau_{10}^*[&\frac{\alpha^2\gamma(1-\delta)^2y_1^*}{(1+\alpha\gamma(1-\delta)x_1^*)^3}-\frac{r}{K}e^{-i\omega_{10}^*\tau_{10}^*}-\frac{\alpha(1-\delta)\Delta}{(1+\alpha\gamma(1-\delta)x_1^*)^2}\\&+\overline{\Delta^*}(\frac{\beta\alpha(1-\delta)\Delta}{(1+\alpha\gamma(1-\delta)x_1^*)^2}e^{-i\omega_{10}^*\tau_2^*}-\frac{\beta\alpha^2\gamma(1-\delta)^2y_1^*}{(1+\alpha\gamma(1-\delta)x_1^*)^3}e^{-2i\omega_{10}^*\tau_2^*}\\&-\frac{pE_1^*w\Delta^2}{(py_1^*-w)^2})],\end{aligned}$$

$$
\begin{aligned}
g_{11} = 2\overline{D}\tau_{10}^*[&\frac{\alpha^2\gamma(1-\delta)^2y_1^*}{(1+\alpha\gamma(1-\delta)x_1^*)^3} - \frac{r}{K}\,Re\{e^{i\omega_{10}^*\tau_{10}^*}\} - \frac{\alpha(1-\delta)\,Re\{\Delta\}}{(1+\alpha\gamma(1-\delta)x_1^*)^2}\\
&+ \overline{\Delta^*}(\frac{\beta\alpha(1-\delta)}{(1+\alpha\gamma(1-\delta)x_1^*)^2}\,Re\{\Delta e^{i\omega_{10}^*\tau_2^*}\} - \frac{\beta\alpha^2\gamma(1-\delta)^2y_1^*}{(1+\alpha\gamma(1-\delta)x_1^*)^3}\\
&- \frac{pE_1^*w\Delta\overline{\Delta}}{(py_1^*-w)^2})],
\end{aligned}
$$

$$
\begin{aligned}
g_{02} = 2\overline{D}\tau_{10}^*[&\frac{\alpha^2\gamma(1-\delta)^2y_1^*}{(1+\alpha\gamma(1-\delta)x_1^*)^3} - \frac{r}{K}e^{i\omega_{10}^*\tau_{10}^*} - \frac{\alpha(1-\delta)\overline{\Delta}}{(1+\alpha\gamma(1-\delta)x_1^*)^2}\\
&+ \overline{\Delta^*}(\frac{\beta\alpha(1-\delta)\overline{\Delta}}{(1+\alpha\gamma(1-\delta)x_1^*)^2}e^{i\omega_{10}^*\tau_2^*} - \frac{\beta\alpha^2\gamma(1-\delta)^2y_1^*}{(1+\alpha\gamma(1-\delta)x_1^*)^3}e^{2i\omega_{10}^*\tau_2^*}\\
&- \frac{pE_1^*w\overline{\Delta}^2}{(py_1^*-w)^2})],
\end{aligned}
$$

$$
\begin{aligned}
g_{21} = 2\overline{D}\tau_{10}^*\{&\frac{\alpha^2\gamma(1-\delta)^2y_1^*}{(1+\alpha\gamma(1-\delta)x_1^*)^3}(2W_{11}^{(1)}(0)+W_{20}^{(1)}(0)) - \frac{r}{K}(W_{11}^{(1)}(-1)\\
&+ \frac{W_{20}^{(1)}(-1)}{2} + \frac{W_{20}^{1}(0)}{2}e^{i\omega_{10}^*\tau_{10}^*} + W_{11}^{(1)}(0)e^{-i\omega_{10}^*\tau_{10}^*})\\
&- \frac{\alpha(1-\delta)}{(1+\alpha\gamma(1-\delta)x_1^*)^2}(W_{11}^{2}(0) + \frac{W_{20}^{(2)}(0)}{2} + \frac{W_{20}^{(1)}(0)}{2}\overline{\Delta} + W_{11}^{(1)}(0)\Delta)\\
&- \frac{3\alpha^3\gamma^2(1-\delta)^3y_1^*}{(1+\alpha\gamma(1-\delta)x_1^*)^4} + \frac{\alpha^2\gamma(1-\delta)^2}{(1+\alpha\gamma(1-\delta)x_1^*)^3}(\overline{\Delta}+2\Delta)\\
&+ \overline{\Delta^*}[\frac{\beta\alpha(1-\delta)}{(1+\alpha\gamma(1-\delta)x_1^*)^2}(W_{11}^{(2)}(0)e^{-i\omega_{10}^*\tau_2^*} + \frac{W_{20}^{(2)}(0)}{2}e^{i\omega_{10}^*\tau_2^*}\\
&+ \frac{W_{20}^{(1)}(-\frac{\tau_2^*}{\tau_{10}^*})}{2}\overline{\Delta} + W_{11}^{(1)}(-\frac{\tau_2^*}{\tau_{10}^*})\Delta) - \frac{\beta\alpha^2\gamma(1-\delta)^2y_1^*}{(1+\alpha\gamma(1-\delta)x_1^*)^3}\\
&\cdot(2W_{11}^{(1)}(-\frac{\tau_2^*}{\tau_{10}^*})e^{-i\omega_{10}^*\tau_2^*} + W_{20}^{(1)}(-\frac{\tau_2^*}{\tau_{10}^*})e^{i\omega_{10}^*\tau_2^*}) - \frac{pE_1^*w}{(py_1^*-w)^2}\\
&\cdot(2W_{11}^{(2)}(0)\Delta + W_{20}^{(2)}(0)\overline{\Delta}) + \frac{3\beta\alpha^3\gamma^2(1-\delta)^3y_1^*}{(1+\alpha\gamma(1-\delta)x_1^*)^4}e^{-i\omega_{10}^*\tau_2^*}\\
&- \frac{\beta\alpha^2\gamma(1-\delta)^2}{(1+\alpha\gamma(1-\delta)x_1^*)^3}(\overline{\Delta}e^{-2i\omega_{10}^*\tau_2^*}+2\Delta) + \frac{3mp^2w\Delta^2\overline{\Delta}}{(py_1^*-w)^4}]\}.
\end{aligned}
$$

We need to compute $W_{20}(\theta)$ and $W_{11}(\theta)$. From (20) and (22), we have

$$
\begin{aligned}
\dot{W} &= \dot{u}_t - \dot{z}q - \dot{\overline{z}}\overline{q}\\
&= \begin{cases} AW - 2\,Re\{\overline{q^*}(0)F_0q(\theta)\}, & -1 \le \theta < 0,\\ AW - 2\,Re\{\overline{q^*}(0)F_0q(\theta)\} + F_0, & \theta = 0, \end{cases}\\
&= AW + H(z,\overline{z},\theta),
\end{aligned}
\tag{25}
$$

where

$$
H(z,\overline{z},\theta) = H_{20}(\theta)\frac{z^2}{2} + H_{11}(\theta)z\overline{z} + H_{02}(\theta)\frac{\overline{z}^2}{2} + \cdots. \tag{26}
$$

Note that on the center manifold C_0 near the origin, we have

$$\dot{W} = W_z\dot{z} + W_{\overline{z}}\dot{\overline{z}}.$$

Substituting the corresponding series into (25) and comparing the coefficients, we have

$$\begin{aligned}(A - 2i\omega_{10}^*\tau_{10}^* I)W_{20}(\theta) &= -H_{20}(\theta),\\ AW_{11}(\theta) &= -H_{11}(\theta).\end{aligned} \tag{27}$$

From (25), we know that for $\theta \in [-1, 0)$

$$H(z, \overline{z}, \theta) = -\overline{q^*}(0)F_0q(\theta) - q^*(0)\overline{F}_0\overline{q}(\theta) = -gq(\theta) - \overline{gq}(\theta). \tag{28}$$

Comparing the coefficients with (26), we obtain

$$\begin{aligned}H_{20}(\theta) &= -g_{20}q(\theta) - \overline{g}_{02}\overline{q}(\theta),\\ H_{11}(\theta) &= -g_{11}q(\theta) - \overline{g}_{11}\overline{q}(\theta).\end{aligned} \tag{29}$$

From (27) and (29) and the definition of A, it follows that

$$\dot{W}_{20}(\theta) = 2i\omega_{10}^*\tau_{10}^*W_{20}(\theta) + g_{20}q(\theta) + \overline{g}_{02}\overline{q}(\theta).$$

Notice that $q(\theta) = q(0)e^{i\omega_{10}^*\tau_{10}^*\theta}$. Hence,

$$W_{20}(\theta) = \frac{ig_{20}}{\omega_{10}^*\tau_{10}^*}q(0)e^{i\omega_{10}^*\tau_{10}^*\theta} + \frac{i\overline{g}_{02}}{3\omega_{10}^*\tau_{10}^*}\overline{q}(0)e^{-i\omega_{10}^*\tau_{10}^*\theta} + M_1e^{2i\omega_{10}^*\tau_{10}^*\theta}, \tag{30}$$

where $M_1 = \left(M_1^{(1)}, M_1^{(2)}\right) \in R^2$ is a constant vector.

Similarly, from (27) and (29), we obtain

$$W_{11}(\theta) = -\frac{ig_{11}}{\omega_{10}^*\tau_{10}^*}q(0)e^{i\omega_{10}^*\tau_{10}^*\theta} + \frac{i\overline{g}_{11}}{\omega_{10}^*\tau_{10}^*}\overline{q}(0)e^{-i\omega_{10}^*\tau_{10}^*\theta} + M_2, \tag{31}$$

where $M_2 = \left(M_2^{(1)}, M_2^{(2)}\right) \in R^2$ is also a constant vector.

In the following we shall find out constant vectors M_1 and M_2. From (25) and (26), we have

$$H_{20}(0) = -g_{20}q(0) - \overline{g}_{02}\overline{q}(0) + 2\tau_{10}^*N_1, \tag{32}$$

$$H_{11}(0) = -g_{11}q(0) - \overline{g}_{11}\overline{q}(0) + 2\tau_{10}^*N_2, \tag{33}$$

where

$$N_1 = \begin{pmatrix} \dfrac{\alpha^2\gamma(1-\delta)^2y_1^*}{(1+\alpha\gamma(1-\delta)x_1^*)^3} - \dfrac{r}{K}e^{-i\omega_{10}^*\tau_{10}^*} - \dfrac{\alpha(1-\delta)\Delta}{(1+\alpha\gamma(1-\delta)x_1^*)^2} \\ \dfrac{\beta\alpha(1-\delta)\Delta e^{-i\omega_{10}^*\tau_2^*}}{(1+\alpha\gamma(1-\delta)x_1^*)^2} - \dfrac{\beta\alpha^2\gamma(1-\delta)^2y_1^*e^{-2i\omega_{10}^*\tau_2^*}}{(1+\alpha\gamma(1-\delta)x_1^*)^3} - \dfrac{pE_1^*w\Delta^2}{(py_1^*-w)^2} \end{pmatrix},$$

$$N_2 = \begin{pmatrix} \dfrac{\alpha^2\gamma(1-\delta)^2y_1^*}{(1+\alpha\gamma(1-\delta)x_1^*)^3} - \dfrac{r}{K}\,Re(e^{i\omega_{10}^*\tau_{10}^*}) - \dfrac{\alpha(1-\delta)\,Re(\Delta)}{(1+\alpha\gamma(1-\delta)x_1^*)^2} \\ \dfrac{\beta\alpha(1-\delta)\,Re(\Delta e^{i\omega_{10}^*\tau_2^*})}{(1+\alpha\gamma(1-\delta)x_1^*)^2} - \dfrac{\beta\alpha^2\gamma(1-\delta)^2y_1^*}{(1+\alpha\gamma(1-\delta)x_1^*)^3} - \dfrac{pE_1^*w\Delta\overline{\Delta}}{(py_1^*-w)^2} \end{pmatrix}.$$

Substituting (30), (31) and (32), (33) into (27) and noticing that

$$\left(i\omega_{10}^{*}\tau_{10}^{*}I - \int_{-1}^{0} e^{i\omega_{10}^{*}\tau_{10}^{*}\theta} d\eta(\theta) \right) q(0) = 0,$$

and

$$\left(-i\omega_{10}^{*}\tau_{10}^{*}I - \int_{-1}^{0} e^{-i\omega_{10}^{*}\tau_{10}^{*}\theta} d\eta(\theta) \right) \overline{q}(0) = 0,$$

we obtain

$$\left(2i\omega_{10}^{*}\tau_{10}^{*}I - \int_{-1}^{0} e^{2i\omega_{10}^{*}\tau_{10}^{*}\theta} d\eta(\theta) \right) M_1 = 2\tau_{10}^{*} N_1,$$

and

$$\int_{-1}^{0} d\eta(\theta) M_2 = -2\tau_{10}^{*} N_2.$$

Therefore, we obtain

$$M_1 = 2 \begin{pmatrix} 2i\omega_{10}^{*} - \dfrac{\alpha^2\gamma(1-\delta)^2 x_1^{*} y_1^{*}}{(1+\alpha\gamma(1-\delta)x_1^{*})^2} + \dfrac{r x_1^{*}}{K} e^{-2i\omega_{10}^{*}\tau_{10}^{*}} & \dfrac{\alpha(1-\delta)x_1^{*}}{1+\alpha\gamma(1-\delta)x_1^{*}} \\ -\dfrac{\beta\alpha(1-\delta)y_1^{*}}{1+\alpha\gamma(1-\delta)x_1^{*}} e^{-2i\omega_{10}^{*}\tau_2^{*}} & 2i\omega_{10}^{*} - \dfrac{pE_1^{*}y_1^{*}}{py_1^{*}-w} \end{pmatrix}^{-1} N_1,$$

and

$$M_2 = 2 \begin{pmatrix} \dfrac{r x_1^{*}}{K} - \dfrac{\alpha^2\gamma(1-\delta)^2 x_1^{*} y_1^{*}}{(1+\alpha\gamma(1-\delta)x_1^{*})^2} & \dfrac{\alpha(1-\delta)x_1^{*}}{1+\alpha\gamma(1-\delta)x_1^{*}} \\ -\dfrac{\beta\alpha(1-\delta)y_1^{*}}{(1+\alpha\gamma(1-\delta)x_1^{*})^2} & -\dfrac{pE_1^{*}y_1^{*}}{py_1^{*}-w} \end{pmatrix}^{-1} N_2.$$

Thus, we can determine $W_{20}(\theta)$ and $W_{11}(\theta)$ from (30) and (31). Furthermore, g_{21} can be expressed by the parameters of system (17). Hence, we can compute the following values:

$$\begin{aligned} c_1(0) &= \frac{i}{2\omega_{10}^{*}\tau_{10}^{*}}\left(g_{20}g_{11} - 2|g_{11}|^2 - \frac{|g_{02}|^2}{3}\right) + \frac{g_{21}}{2}, \\ \mu_2 &= -\frac{Re\{c_1(0)\}}{Re\{\lambda'(\tau_{10}^{*})\}}, \\ \beta_2 &= 2\,Re\{c_1(0)\}, \\ T_2 &= -\frac{Im\{c_1(0)\} + \mu_2\, Im\{\lambda'(\tau_{10}^{*})\}}{\omega_{10}^{*}\tau_{10}^{*}}. \end{aligned}$$

From the conclusion of Hassard et al. [10], we have the following results.

Theorem 5. *μ_2 determines the direction of the Hopf bifurcation: if $\mu_2 > 0$ ($\mu_2 < 0$), the Hopf bifurcation is supercritical (subcritical); β_2 determines the stability of the bifurcating periodic solution: the bifurcating periodic solution is stable (unstable) if $\beta_2 < 0$ ($\beta_2 > 0$) and T_2 determines the period of the bifurcating periodic solution: the period increases (decreases) if $T_2 > 0$ ($T_2 < 0$).*

4. Effect of fluctuating environment

In this section we consider the growth of the prey population and natural mortality of the predator population in a stochastic environment by incorporating white noise in each of the equations of system (3), leading to:

$$\begin{cases} \dfrac{dx}{dt} = (r + \xi_1(t))x - \dfrac{rxx(t-\tau_1)}{K} - \dfrac{\alpha(1-\delta)xy}{1+\alpha\gamma(1-\delta)x}, \\ \dfrac{dy}{dt} = \dfrac{\beta\alpha(1-\delta)x(t-\tau_2)y}{1+\alpha\gamma(1-\delta)x(t-\tau_2)} + (-d + \xi_2(t))y - Ey, \\ E(py - w) - m = 0, \end{cases} \tag{34}$$

where the environmental parameters r and d have been perturbed by mutually independent white noise characterized by

$$\bar{\xi}_1(t) = 0, \qquad \bar{\xi}_2(t) = 0,$$
$$\overline{\xi_i(t_1)\xi_j(t_2)} = \delta_{ij}\delta(t_1 - t_2), \quad i, j = 1, 2,$$

where the bar represents the ensemble average of random environment, δ_{ij} is the Kronecker delta denoting the spectral density of the white noise and δ is the Dirac delta function with distinct times t_1 and t_2.

Introducing a transformation of the form $x = x^*e^{\eta_1(t)}$ and $y = y^*e^{\eta_2(t)}$ in system (34) and neglecting the second and higher terms, we transform this system into the following normal form:

$$\begin{cases} \dfrac{d\eta_1}{dt} = \xi_1(t) + \dfrac{\alpha^2\gamma(1-\delta)^2x^*y^*}{(1+\alpha\gamma(1-\delta)x^*)^2}\eta_1 - \dfrac{rx^*}{K}\eta_1(t-\tau_1) - \dfrac{\alpha(1-\delta)y^*}{1+\alpha\gamma(1-\delta)x^*}\eta_2, \\ \dfrac{d\eta_2}{dt} = \xi_2(t) + \dfrac{\beta\alpha(1-\delta)x^*}{(1+\alpha\gamma(1-\delta)x^*)^2}\eta_1(t-\tau_2) + \dfrac{pmy^*}{(py^* - w)^2}\eta_2. \end{cases} \tag{35}$$

Consider a continuous function $X(t)$ in the interval $-T/2 \le t \le T/2$ and its Fourier transform $\tilde{X}(\omega)$

$$\tilde{X}(\omega) = \int_{-\frac{T}{2}}^{\frac{T}{2}} X(t)e^{-i\omega t}dt,$$
$$X(t) = \frac{1}{2\pi}\int_{-\infty}^{+\infty} \tilde{X}(\omega)e^{i\omega t}d\omega.$$

Hence, the Fourier transform of the system (35) can be expressed as

$$\begin{cases} \tilde{\xi}_1(\omega) = (i\omega - \dfrac{\alpha^2\gamma(1-\delta)^2x^*y^*}{(1+\alpha\gamma(1-\delta)x^*)^2} + \dfrac{rx^*}{K}e^{-i\omega\tau_1})\tilde{\eta}_1(\omega) + \dfrac{\alpha(1-\delta)y^*}{1+\alpha\gamma(1-\delta)x^*}\tilde{\eta}_2(\omega), \\ \tilde{\xi}_2(\omega) = -\dfrac{\beta\alpha(1-\delta)x^*}{(1+\alpha\gamma(1-\delta)x^*)^2}e^{-i\omega\tau_2}\tilde{\eta}_1(\omega) + (i\omega - \dfrac{pmy^*}{(py^* - w)^2})\tilde{\eta}_2(\omega), \end{cases} \tag{36}$$

where $\tilde{\xi}_i$ and $\tilde{\eta}_i$, $i = 1, 2$ denote the Fourier transform of ξ_i and η_i, $i = 1, 2$ respectively. For the sake of simplicity, we rewrite system (36) into the following matrix form:

$$\begin{pmatrix} \tilde{\xi}_1(\omega) \\ \tilde{\xi}_2(\omega) \end{pmatrix} = \begin{pmatrix} i\omega - p_{111} - p_{112}e^{-i\omega\tau_1} & -p_{12} \\ -p_{21}e^{-i\omega\tau_2} & i\omega - p_{22} \end{pmatrix} \begin{pmatrix} \tilde{\eta}_1(\omega) \\ \tilde{\eta}_2(\omega) \end{pmatrix}, \tag{37}$$

where

$$\begin{aligned} p_{111} &= \frac{\alpha^2\gamma(1-\delta)^2x^*y^*}{1+\alpha\gamma(1-\delta)x^*}, \\ p_{112} &= -\frac{rx^*}{K}, \\ p_{12} &= -\frac{\alpha(1-c)y^*}{1+\alpha\gamma(1-\delta)x^*}, \\ p_{21} &= \frac{\beta\alpha(1-\delta)x^*}{(1+\alpha\gamma(1-\delta)x^*)^2}, \\ p_{22} &= \frac{pmy^*}{(py^*-w)^2}. \end{aligned}$$

Then

$$\tilde{\eta}_i(\omega) = \sum_{j=1}^{2} b_{ij}\tilde{\xi}_j(\omega), \quad i = 1, 2,$$

where $\begin{pmatrix} b_{11} & b_{12} \\ b_{21} & b_{22} \end{pmatrix} = \begin{pmatrix} i\omega - p_{111} - p_{112}e^{-i\omega\tau_1} & -p_{12} \\ -p_{21}e^{-i\omega\tau_2} & i\omega - p_{22} \end{pmatrix}^{-1}$.

If the function $X(t)$ has zero mean value, the fluctuation intensity of the components in the frequency band ω and $\omega + d\omega$ is $S_X(\omega)d\omega$ formally defined as

$$S_X(\omega)d\omega = \lim_{T\to\infty} \frac{\overline{|\tilde{X}(\omega)|^2}}{T}.$$

Thus

$$\begin{aligned} S_\xi(\omega)d\omega &= \lim_{T\to\infty} \frac{\overline{|\tilde{\xi}(\omega)|^2}}{T} \\ &= \lim_{T\to\infty} \frac{1}{T} \int_{-\frac{T}{2}}^{\frac{T}{2}} \int_{-\frac{T}{2}}^{\frac{T}{2}} \overline{\xi(s)\xi(s')} e^{i\omega(s'-s)} ds ds'. \end{aligned}$$

And the following equations can be obtained:

$$S_{\eta_i}(\omega) = \sum_{j=1}^{2} |b_{ij}|^2 S_{\xi_j}(\omega).$$

Therefore, the fluctuation intensity in η_i is given by

$$\begin{aligned}\sigma_{\eta_i}^2 =&\frac{1}{2\pi}\int_{-\infty}^{\infty} S_{\eta_i}(\omega)d\omega\\ =&\frac{1}{2\pi}\sum_{j=1}^{2}\int_{-\infty}^{\infty}|b_{ij}|^2 S_{\xi_j}(\omega)d\omega\\ =&\frac{1}{2\pi}\int_{-\infty}^{\infty}\frac{T_i(\omega)}{B(\omega)}d\omega,\quad i=1,2,\end{aligned}\tag{38}$$

where

$$\begin{aligned}&T_1(\omega)=p_{22}^2+\omega^2+p_{12}^2,\\ &T_2(\omega)=p_{21}^2+p_{111}^2+p_{112}^2+\omega^2+2p_{111}p_{112}\cos(\omega\tau_1)+2\omega p_{112}\sin(\omega\tau_1),\\ &B(\omega)=[(p_{111}+p_{112}\cos(\omega\tau_1))p_{22}-\omega(\omega+p_{112}\sin(\omega\tau_1))-p_{12}p_{21}\cos(\omega\tau_2)]^2\\ &\qquad+[p_{22}(\omega+p_{112}\sin(\omega\tau_1))+\omega(p_{111}+p_{112}\cos(\omega\tau_1))-p_{12}p_{21}\sin(\omega\tau_2)]^2.\end{aligned}$$

In the presence of environmental fluctuation, integral computation of equation (38) makes it difficult to obtain an explicit form of the spectral densities of prey and predator populations. Hence, we will compute the population fluctuation intensity with numerical simulations.

5. Optimal harvesting

To maximize economic profit and ensure the population persistence, we discuss optimal harvesting strategy for system (3) without time delays. Due to instantaneous annual discount rate ϵ, this optimal problem can be described as

$$m(E)=\int_{t_0}^{t_f}E(py-w)e^{-\epsilon t}dt,$$

subjected to system (3) and harvesting constraint

$$0\le E(t)\le E^{max}.$$

Let x^{opt}, y^{opt} and E^{opt} be the optimal population densities and the corresponding optimal harvesting rate, respectively. Our objective is to determine optimal harvesting E^{opt} such that

$$m(E^{opt})=\max\{m(E):E(t)\in[0,E^{max}]\}.$$

In order to find optimal values, we construct the Hamiltonian function as follows:

$$\begin{aligned}H=&E(py-w)e^{-\epsilon t}+\sigma_1[rx(1-\frac{x}{K})-\frac{\alpha(1-\delta)xy}{1+\alpha\gamma(1-\delta)x}]\\ &+\sigma_2[\frac{\beta\alpha(1-\delta)xy}{1+\alpha\gamma(1-\delta)x}-dy-Ey],\end{aligned}$$

where $\sigma_1(t)$ and $\sigma_2(t)$ are adjoint variables.

The partial derivative of the Hamiltonian function H with respect to the harvesting effort can be computed as

$$\frac{\partial H}{\partial E} = (py - w)e^{-\epsilon t} - \sigma_2 y = D_E H(t),$$

where the term $D_E H(t)$ is called the switching function. The sign of the switching function $D_E H(t)$ determines optimal harvesting $E(t)$ as a bang–bang control problem, i.e., changing from one level 0 to the other E^{max}. When $D_E H(t) = 0$, the Hamiltonian function H becomes independent of harvesting $E(t)$. In this case, it is a singular control problem. Hence, the optimal harvesting solution is

$$E(t) = \begin{cases} E^{max} & \text{if} \quad D_E H(t) > 0, \\ 0 & \text{if} \quad D_E H(t) < 0, \\ E^{opt} & \text{if} \quad D_E H(t) = 0. \end{cases}$$

For the case of a singular control, we now present the expression of E^{opt}. When $D_E H(t) = 0$, we have

$$\sigma_2(t) = e^{-\epsilon t}(p - \frac{w}{y}). \tag{39}$$

Using the Pontryagin's Maximum Principle, the adjoint variables $\sigma_1(t)$ and $\sigma_2(t)$ satisfy the following equations:

$$\begin{aligned} \frac{d\sigma_1}{dt} &= -\frac{\partial H}{\partial x} = (\frac{rx}{K} - \frac{\gamma\alpha^2(1-\delta)^2 xy}{(1+\alpha\gamma(1-\delta)x)^2})\sigma_1 - \frac{\beta\alpha(1-\delta)y}{(1+\alpha\gamma(1-\delta)x)^2}\sigma_2, \\ \frac{d\sigma_2}{dt} &= -\frac{\partial H}{\partial y} = -pEe^{-\epsilon t} + \frac{\alpha(1-\delta)x}{1+\alpha\gamma(1-\delta)x}\sigma_1. \end{aligned} \tag{40}$$

To solve equation (40), we transfer it into the following second-order ordinary differential equation:

$$\frac{d^2\sigma_1}{dt^2} + L_1\frac{d\sigma_1}{dt} + L_2\sigma_1 = G_1 e^{-\epsilon t}, \tag{41}$$

where

$$\begin{aligned} L_1 &= -\frac{rx}{K} + \frac{\gamma\alpha^2(1-\delta)^2 xy}{(1+\alpha\gamma(1-\delta)x)^2}, \\ L_2 &= \frac{\beta\alpha^2(1-\delta)^2 xy}{(1+\alpha\gamma(1-\delta)x)^3}, \\ G_1 &= \frac{p\beta\alpha(1-\delta)yE}{(1+\alpha\gamma(1-\delta)x)^2}. \end{aligned}$$

In order to remain the shadow price $\sigma_1 e^{\epsilon t}$ bounded, we neglect the integration constant of equation (41) and obtain $\sigma_1(t) = C_1 \exp(-\epsilon t)$, where $C_1 = G_1/(\epsilon^2 - L_1\epsilon + L_2)$.

By a similar computation, we can also obtain $\sigma_2(t) = C_2 \exp(-\epsilon t)$, where $C_2 = G_2/(\epsilon^2 - L_1\epsilon + L_2)$, $G_2 = pE(\epsilon + rx/K - \gamma\alpha^2(1-\delta)^2 xy/(1+\alpha\gamma(1-\delta)x)^2)$. Combined with equation (39), the optimal harvesting rate takes the following form:

$$E = \frac{(\epsilon^2 - L_1\epsilon + L_2)(py - w)}{py(\epsilon - L_1)}. \tag{42}$$

Hence, we can find the optimal equilibrium populations (x^{opt}, y^{opt}) and optimal harvesting rate E^{opt} by the solving biological equilibrium together with equation (42).

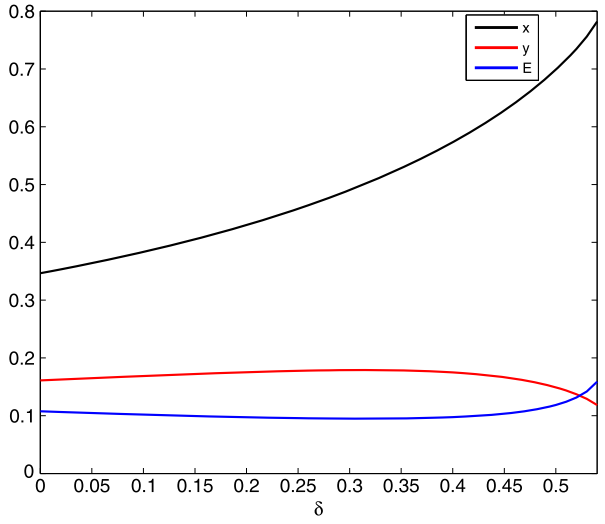

Fig. 1. Numerical simulations of the positive equilibrium (x, y, E) when varying $\delta \in (0, 0.54)$.

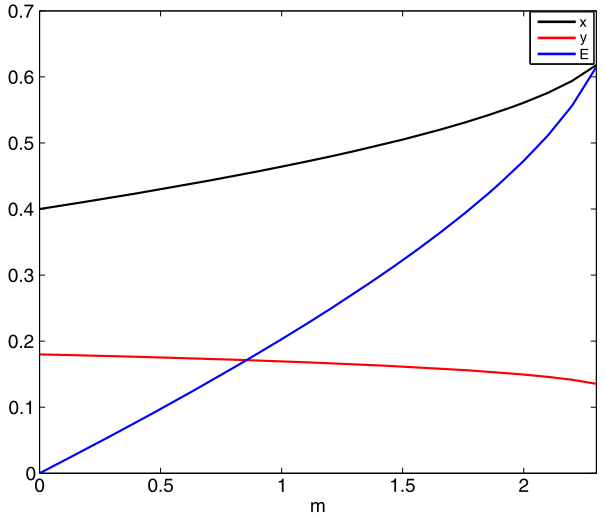

Fig. 2. Numerical simulations of the positive equilibrium (x, y, E) when varying $m \in (0, 2.3)$.

6. Numerical simulations

We illustrate the insights of our theoretical analysis through intensive simulations on the following system:

$$\begin{cases} \dfrac{dx}{dt} = x(1 - x(t - \tau_1)) - \dfrac{6.25(1-\delta)xy}{1 + 1.5625(1-\delta)x}, \\ \dfrac{dy}{dt} = \dfrac{9.375(1-\delta)x(t-\tau_2)y}{1 + 1.5625(1-\delta)x(t-\tau_2)} - 2y - Ey, \\ 0 = E(35y - 1) - m. \end{cases} \tag{43}$$

In this model, corresponding to model (3), we take $r = 1$; $K = 1$; $\alpha = 6.25$; $\gamma = 0.25$; $\beta = 1.5$; $d = 2$; $p = 35$; $w = 1$. When the parameter $m = 0.5$ is fixed, model (43) admits a positive equilibrium for $\delta \in (0, 0.54)$ (see Fig. 1). When the parameter $\delta = 0.2$ is fixed, model (43) admits a positive equilibrium for $m \in (0, 2.3)$ (see Fig. 2). From these two figures, we know that the prey density x and harvesting rate E are strictly increasing functions of δ and m, whereas the predator density y is decreasing, i.e., the habitat complexity

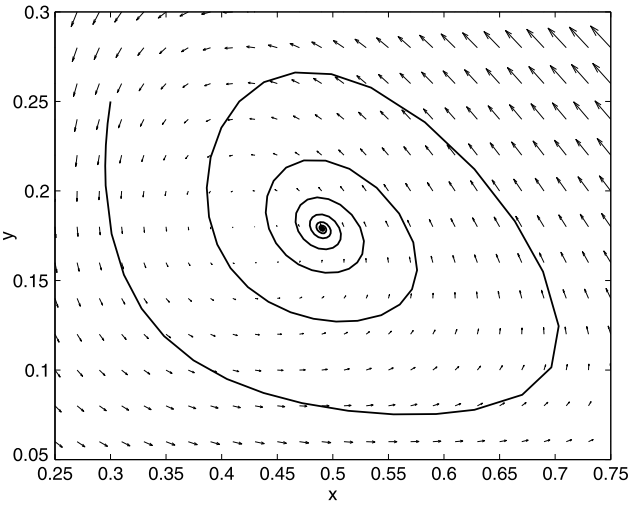

Fig. 3. In absence of delay, the positive equilibrium P of model (43) is asymptotically stable.

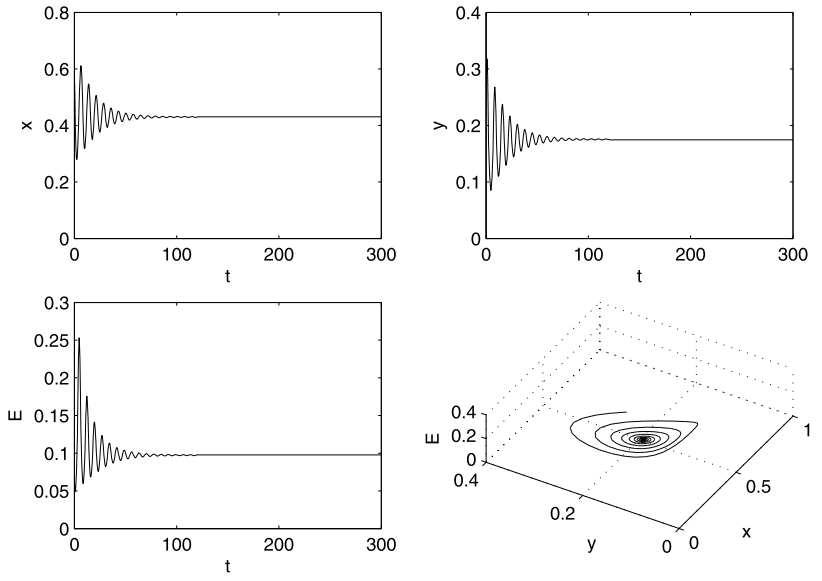

Fig. 4. Without any time delay, positive equilibrium point P is asymptotically stable.

and economic profit of harvesting have positive impact on the prey but negative impact on the predator species.

Next, we consider the case for the fixed $\delta = 0.2$ and $m = 0.5$. In the absence of delay, $P(0.4299, 0.1753, 0.0974)$ is a positive equilibrium point of model (43). The dynamic behaviors of species x and y are described in Fig. 3, which demonstrates the asymptotic stability of the equilibrium. In Fig. 4, we display the density of (x, y, E) as functions of time, and the phase portrait of model (43) with the initial condition $(0.6, 0.25, 0.1)$.

Obviously, $A_2 + A_4 - A_5 = -0.8046 < 0$. Matlab calculations can be used to find the unique positive solution $\omega_{20} = 0.8629$ of equation (10). Thus, in the absence of delay τ_1, the critical value of delay τ_2 defined by (12) is 0.1470, i.e., the positive equilibrium P is asymptotically stable when $0 \leq \tau_2 < \tau_{20} = 0.1470$ and unstable when $\tau_2 > \tau_{20}$, and model (43) undergoes a Hopf bifurcation at the equilibrium P when τ_2 crosses through the critical values τ_{20}, see Fig. 5. In the absence of delay τ_2, the critical delay for τ_1 can be obtained as 0.8001 by a similar computation.

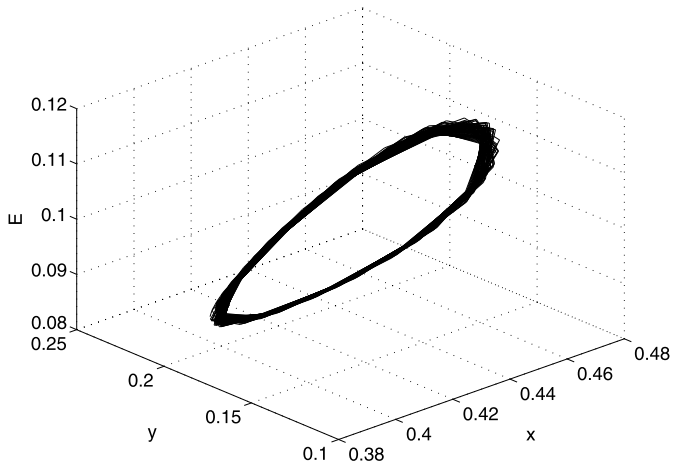

Fig. 5. When $\tau_2 = 0.15 > \tau_{20}$, a periodic solution bifurcating from the equilibrium point P occurs.

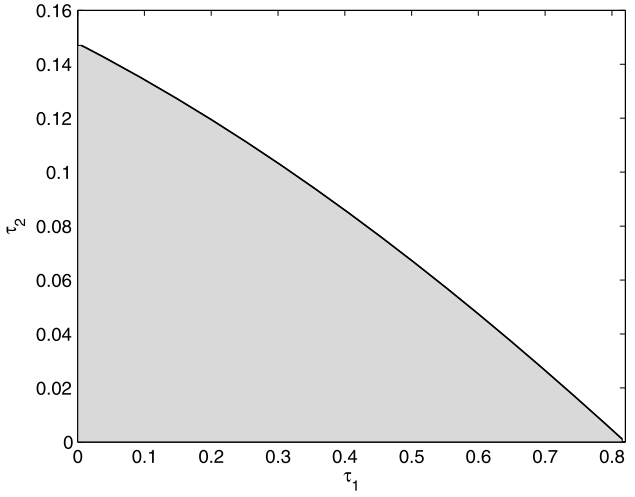

Fig. 6. The stability region in the plane τ_1–τ_2.

For model (43), our analysis for Cases 3 and 4 provides a guide to draw a critical curve $\tau_2 = f(\tau_1)$ w.r.t. two parameters τ_1 and τ_2 (see Fig. 6), i.e., when $\tau_2 \in (0, \tau_{20})$ ($\tau_1 \in (0, \tau_{10})$) is fixed, one can find the critical values τ_{10}^* (τ_{20}^*). Fig. 6 draws the stability region, i.e., the shadow enclosed by curve $f(\tau_1)$ and two axes.

For the fixed delay $\tau_2 = 0.1$, based on our analysis in Section 3, we have $\omega_{10}^* = 0.9879$, $\tau_{10}^* = 0.3198$, $\lambda'(\tau_{10}^*) = 0.1226 + 0.2460i$, $c_1(0) = -1.5550 - 0.4417i$, $\mu_2 = 12.6823$, $\beta_2 = -3.11$, $T_2 = -4.8846$. According to Theorem 5, model (43) undergoes a supercritical Hopf bifurcation at the positive equilibrium P and the bifurcating periodic solution exists for τ_1 slightly larger than τ_{10}^* and the bifurcated periodic solution is stable, as depicted in Fig. 7. Note that for the fixed two time delays τ_1, τ_2 and other parameters referred above, with the increasing of habitat complexity δ, model (43) undergoes dynamics change from an unstable situation to a Hopf bifurcation, and then stabilization finally. This process is illustrated in Fig. 7 and Fig. 8.

We now consider the stochastic delay differential equation model with the same parametric values as in equation (43). In the absence of a gestation delay, Fig. 9 shows stochastically stable population distribution for prey and predator species. In the presence of gestation delays, stochastic effects can be illustrated by increasing the magnitude of the delay. Fig. 10 plots the solutions of the stochastic delay differential model with different delays $\tau_1 = 0.1$, $\tau_2 = 0.1$ and $\tau_1 = 0.3198$, $\tau_2 = 0.15$. This demonstrates that the amplitude of fluctuation increases and the model becomes unstable as time delay increases gradually. Vari-

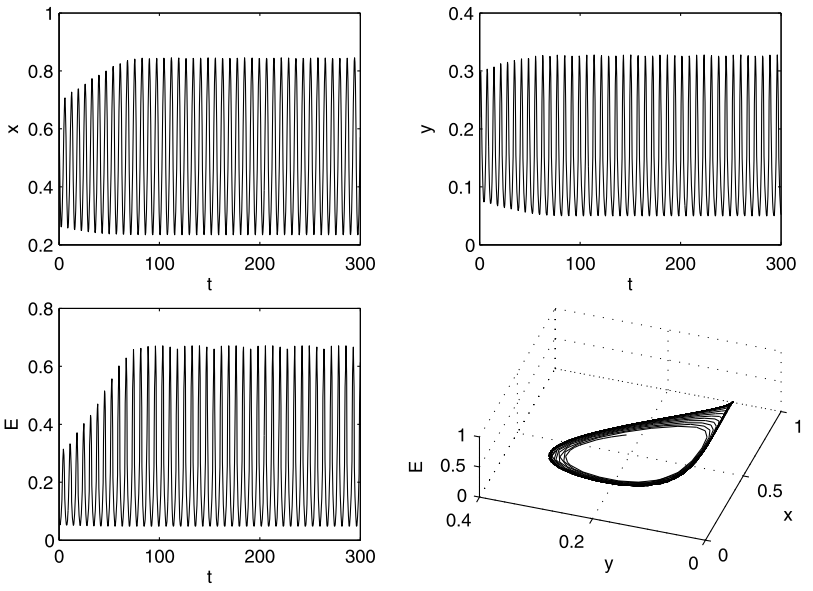

Fig. 7. When $\tau_1 = \tau_{10}^* = 0.3198$ and $\tau_2^* = 0.1$, a periodic solution of model (43) bifurcates from the equilibrium point P occurs.

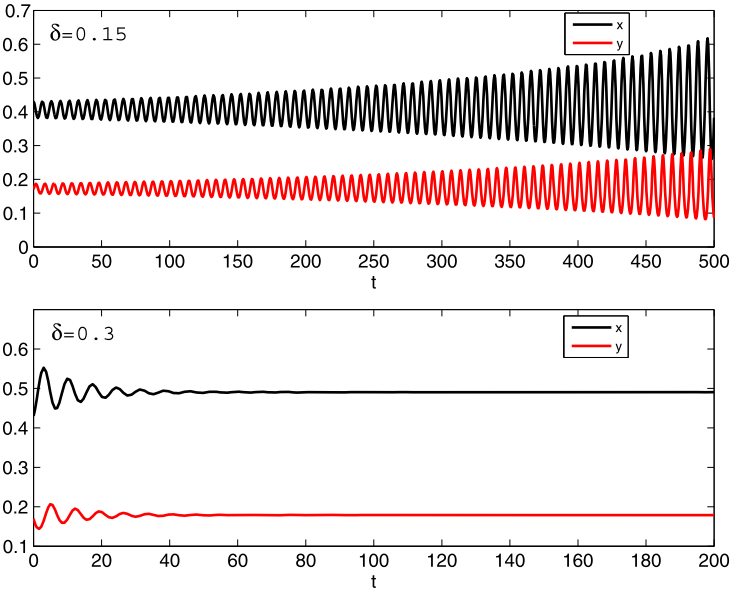

Fig. 8. Plots of (x, y) as functions of the time for different harvest complexity parameter values $\delta = 0.15$ and $\delta = 0.3$.

ations of spectral densities of prey and predator populations with respect to time delay τ_1 are presented in Fig. 11.

For the optimal harvesting consideration, we choose the instantaneous annual discount rate as $\epsilon = 0.01$. The optimal equilibrium populations (x^{opt}, y^{opt}) and optimal harvesting efforts E^{opt} are plotted in Fig. 12. It is clear that the corresponding optimal prey population gradually increases and optimal predator population and the harvesting rate gradually decrease as habitat complexity δ increases. This phenomenon is expected since the impact of habitat complexity on prey is stronger. From Fig. 12, the optimal harvesting rate is near zero when the habitat complexity $\delta = 0.665$. This means that when habitat complexity is beyond the level 0.665, harvesting behavior should not be conducted in order to prevent the predator from extinction.

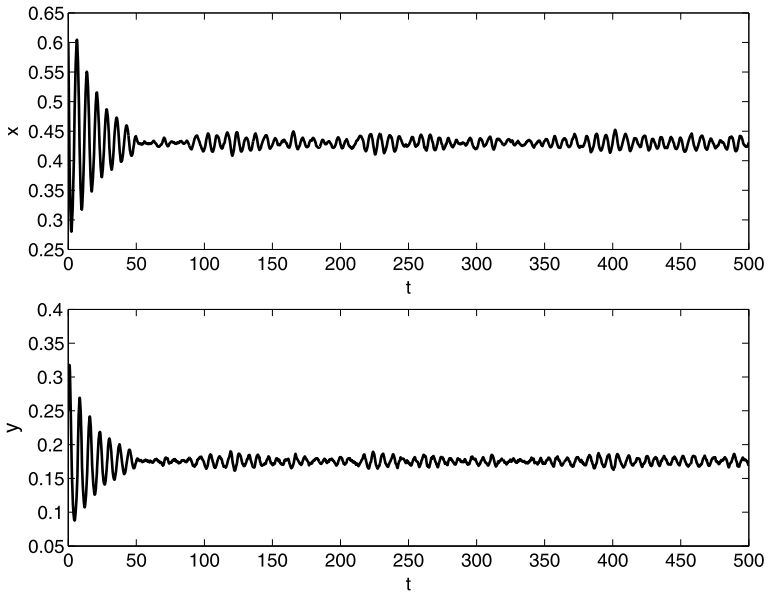

Fig. 9. Solution of the stochastic model (43) in the absence of time delays.

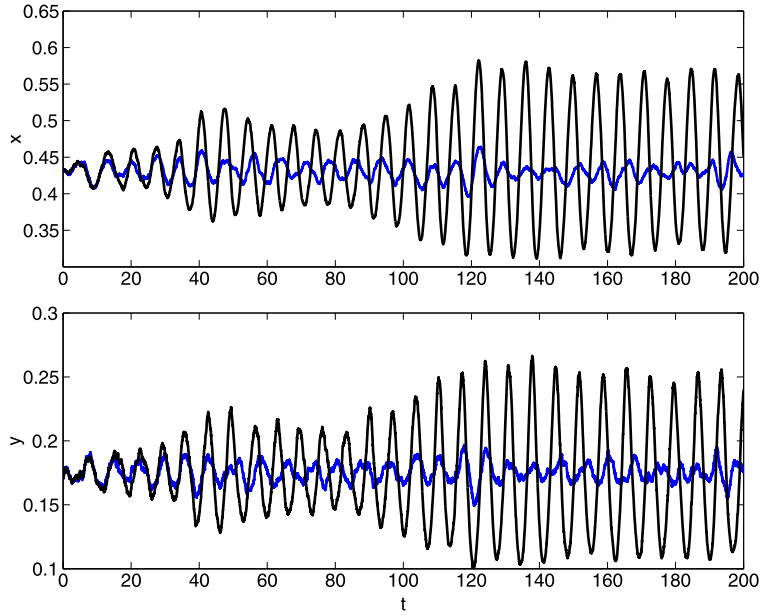

Fig. 10. Solutions of the stochastic delay differential model (43) with different delays $\tau_1 = 0.1$, $\tau_2 = 0.1$ (blue solid line) and $\tau_1 = 0.3198$, $\tau_2 = 0.15$ (black solid line). (For interpretation of the references to color in this figure legend, the reader is referred to the web version of this article.)

7. Conclusions

As pointed in such studies as [13,1], the dynamics of local interacting populations largely depend upon attributes of local habitats. Moreover, it has been reported form some laboratory experiments [2,6,9] that habitat complexity reduces predation rates by decreasing encounter rates between predator and prey. This habitat complexity, largely ignored in existing studies of predator–prey systems, is the main focus of our current study where we considered a delayed differential–algebraic predator–prey model incorporating a parameter characterizing the habitat complexity. More precisely, in our model, the attack coefficient α

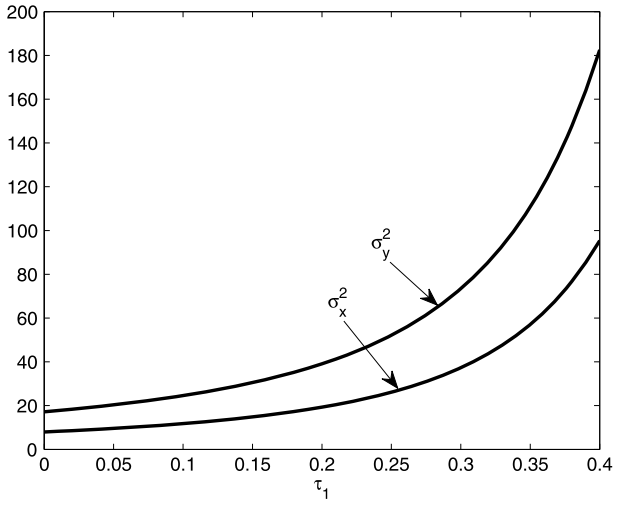

Fig. 11. For the fixed time delay $\tau_2 = 0.01$, spectral density functions vary with increasing time delay $\tau_1 \in (0, 0.4)$.

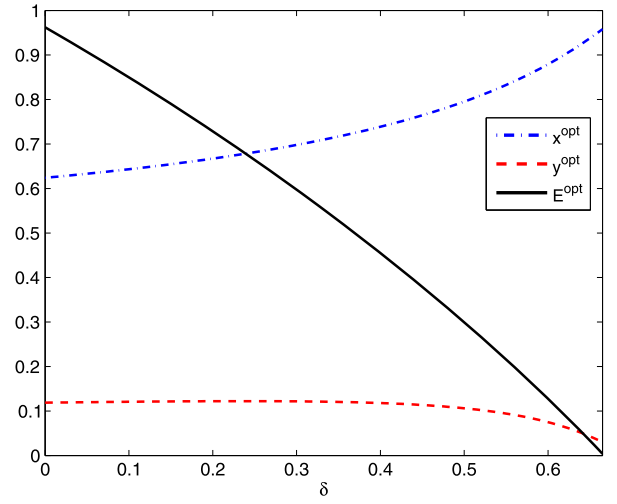

Fig. 12. Optimal equilibrium populations and optimal harvesting rate with respect to habitat complexity $\delta \in (0, 0.665)$.

is replaced by $\alpha(1 - \delta)$, with δ measuring how much encounter rate is reduced due to habitat complexity.

Our work examined the stability region characterized by two time delays: τ_1, the delay relevant to the slow food replacement of the prey population; and τ_2, the gestation delay of the predator. We also, by fixing time delay τ_2, and varying τ_1 as a bifurcation parameter, obtained the direction of Hopf bifurcation and stability of the bifurcated periodic orbit using the normal form and center manifold theories. This analysis then guided us in designing the numerical simulations to demonstrate the effects of habitat complexity on predator–prey interaction with delayed self-limitation and delayed convection to the growth of the predator. We concluded that as the habit complexity increases, it is more difficult for the predator to catch prey and hence habitat complexity provides opportunities for the survival of prey species, and hence more food becomes available later for the predator.

We also examined the stochastic behavior of the delayed differential–algebraic biological system by introducing fluctuations in the growth rate of prey and mortality rate of predator. By using Fourier transform methods, we computed the spectral densities of prey and predator population and we conducted the numerical simulations to illustrate that the spectral density is an increasing function with respect to time

delay, i.e., fluctuation of population density increases as gestation delay increases. We also noted that, in comparison with the deterministic system, it is easier for the stochastic system to drive population densities from being stable to unstable.

We further considered the modelling issue how to balance between the maximum of economic profit and the sustainable development of biological resources. Using the Pontryagin's Maximum Principle, we derived the optimal harvesting strategy. We found that the optimal harvesting will gradually decrease as the strength of habitat complexity increases. In combined, through both mathematical analysis and numerical simulations, we demonstrated that it is possible to achieve the balance of economic profit and environment sustainability by optimizing the harvesting policy.

There are many topics remaining to refine our modelling and furthering the analysis. These include incorporating stage-structure, mutual interference and refuge for the biological relevance; and full bifurcation scenario and global stability analysis for the mathematical details.

Acknowledgments

This work was supported by the Fundamental Research Funds for the Central Universities of China (N140504005), Liaoning's Doctor Startup Fund of China (20131026), China Scholarship Council (201308210128), and the Natural Sciences and Engineering Research Council of Canada (105588-2011-RGPIN). We would like to thank a reviewer for very constructive comments.

References

[1] T.W. Anderson, Predator responses, prey refuges and density-dependent mortality of a marine fish, Ecology 82 (2001) 245–257.
[2] C.R. Canion, K.L. Heck, Effect of habitat complexity on predation success: re-evaluating the current paradigm in seagrass beds, Mar. Ecol. Prog. Ser. 393 (2009) 37–46.
[3] K. Chakraborty, M. Chakraborty, T.K. Kar, Bifurcation and control of a bioeconomic model of a prey–predator system with a time delay, Nonlinear Anal. Hybrid Syst. 5 (2011) 613–625.
[4] B.S. Chen, J.J. Chen, Bifurcation and chaotic behavior of a discrete singular biological economic system, Appl. Math. Comput. 219 (2012) 2371–2386.
[5] B. Christensen, L. Persson, Species-specific antipredator behaviours: effects on prey choice in different habitats, Behav. Ecol. Sociobiol. 32 (1993) 1–9.
[6] S.S. Frederick, P. John, M.C.F. Manderson, The effects of seafloor habitat complexity on survival of juvenile fishes: species-specific interactions with structural refuge, J. Exp. Mar. Biol. Ecol. 335 (2006) 167–176.
[7] H.I. Freedman, V. Sree Hari Rao, The trade-off between mutual interference and time lags in predator–prey systems, Bull. Math. Biol. 45 (1983) 991–1003.
[8] S. Gakkhar, K. Negi, S.K. Sahani, Effects of seasonal growth on ratio dependent delayed prey predator system, Commun. Nonlinear Sci. Numer. Simul. 14 (2009) 850–862.
[9] J.H. Grabowski, S.P. Powers, Habitat complexity mitigates trophic transfer on oyster reefs, Mar. Ecol. Prog. Ser. 277 (2004) 291–295.
[10] B.D. Hassard, N.D. Kazarinoff, Y.H. Wan, Theory and Applications of Hopf Bifurcation, Cambridge University Press, Cambridge, 1981.
[11] C.S. Holling, Some characteristics of simple types of predation and parasitism, Can. Entomol. 91 (1959) 385–398.
[12] H. Huo, W. Li, J. Nieto, Periodic solutions of delayed predator–prey model with the Beddinton–DeAngelis functional response, Chaos Solitons Fractals 33 (2007) 505–512.
[13] W.D. Johnson, Predation, habitat complexity and variation in density dependent mortality of temperate reef fishes, Ecology 87 (2006) 1179–1188.
[14] B. Leonid, E. Braverman, Stability analysis and bifurcations in a diffusive predator–prey system, Discrete Contin. Dyn. Syst. Supplement 2009 (2009) 92–100.
[15] M. Liao, X. Tang, C. Xu, Bifurcation analysis for a three-species predator–prey system with two delays, Commun. Nonlinear Sci. Numer. Simul. 17 (2012) 183–194.
[16] Y. Ma, Global Hopf bifurcation in the Leslie–Gower predator–prey model with two delays, Nonlinear Anal. Real World Appl. 13 (2012) 370–375.
[17] J. Manatunge, T. Asaeda, T. Priyadarshana, The influence of structural complexity on fish–zooplankton interactions: a study using artificial submerged macrophytes, Environ. Biol. Fishes 58 (2000) 425–438.
[18] D. Pal, G.S. Mahaptra, G.P. Samanta, Optimal harvesting of prey–predator system with interval biological parameters: a bioeconomic model, Math. Biosci. 241 (2013) 181–187.
[19] J.F. Savino, R.A. Stein, Behavior of fish predators and their prey: habitat choice between open water and dense vegetation, Environ. Biol. Fishes 24 (1989) 287–293.

[20] S. Shabani, Diffusive Holling type-II predator–prey system with harvesting of prey, J. Math. Anal. Appl. 410 (2014) 469–482.
[21] Y. Song, Y. Peng, J. Wei, Bifurcations for a predator–prey system with two delays, J. Math. Anal. Appl. 337 (2008) 466–479.
[22] S. Tang, J. Liang, Global qualitative analysis of a non-smooth Gause predator–prey model with a refuge, Nonlinear Anal. 76 (2013) 165–180.
[23] M. Vasilova, Asymptotic behavior of a stochastic Gilpin–Ayala predator–prey system with time-dependent delay, Math. Comput. Modelling 57 (2013) 764–781.
[24] S. Yuan, Y. Song, Bifurcation and stability analysis for a delayed Leslie Gower predator–prey system, IMA J. Appl. Math. 74 (2009) 574–603.
[25] G. Zhang, F. Wang, J. Nieto, Complexity of a delayed predator–prey model with impulsive harvest and Holling type II functional response, Adv. Complex Syst. 11 (2008) 77–97.
[26] X. Zhang, Q. Zhang, C. Liu, Z.Y. Xiang, Bifurcation of a singular prey predator economic model with time delay and stage structure, Chaos Solitons Fractals 42 (2009) 1485–1494.
[27] G.D. Zhang, L.L. Zhu, B.S. Chen, Hopf bifurcation and stability for a differential–algebraic biological economic system, Appl. Math. Comput. 217 (2010) 330–338.